

See discussions, stats, and author profiles for this publication at: <https://www.researchgate.net/publication/235650885>

Two-Fluid Model for the Interpretation of Quartz-Crystal Microbalance Response: Tuning Properties of Polymer-Brushes with Solvent Mixtures

ARTICLE in THE JOURNAL OF PHYSICAL CHEMISTRY C · FEBRUARY 2013

Impact Factor: 4.77 · DOI: 10.1021/jp310811a

CITATIONS

5

READS

58

6 AUTHORS, INCLUDING:



Leonid I Daikhin

Tel Aviv University

64 PUBLICATIONS 1,348 CITATIONS

SEE PROFILE



Michael Urbakh

Tel Aviv University

115 PUBLICATIONS 2,108 CITATIONS

SEE PROFILE



Nicholas D Spencer

ETH Zurich

403 PUBLICATIONS 11,621 CITATIONS

SEE PROFILE

Two-Fluid Model for the Interpretation of Quartz Crystal Microbalance Response: Tuning Properties of Polymer Brushes with Solvent Mixtures

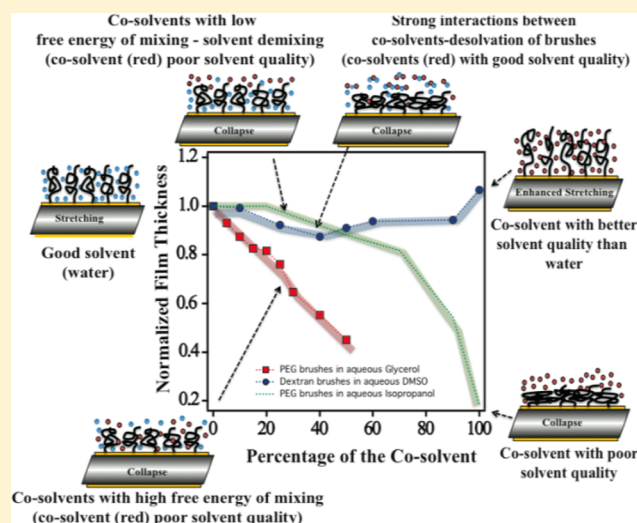
Prathima C. Nalam,^{†,||,§} Leonid Daikhin,^{‡,§} Rosa M. Espinosa-Marzal,[†] Jarred Clasohm,[†] Michael Urbakh,[‡] and Nicholas D. Spencer^{*,†}

[†]Laboratory for Surface Science and Technology, Department of Materials, ETH Zurich, Wolfgang-Pauli-Strasse 10, CH-8093 Zurich, Switzerland

[‡]School of Chemistry, Raymond and Beverly Sackler Faculty of Exact Sciences, Tel-Aviv University, 69978 Ramat-Aviv, Tel Aviv, Israel

Supporting Information

ABSTRACT: A new approach, involving a two-fluid model, has been developed to interpret the quartz crystal microbalance response of adsorbed viscoelastic polymers. The model utilizes the Navier–Stokes–Brinkmann equation to describe the motion of a porous, semirigid, viscoelastic polymer-brush film with a viscous solvent flowing through it. The two phases, solid (polymer brush) and liquid (solvent mixture), hydrodynamically interact with each other, as represented by means of a Darcy term with a characteristic correlation factor. The two-fluid model is used to estimate structural changes in polymer brushes consisting of the copolymers poly(L-lysine)-graft-poly(ethylene glycol) (PLL-g-PEG) or poly(L-lysine)-graft-dextran (PLL-g-dextran) adsorbed on an amorphous SiO₂-coated quartz surface in aqueous solutions of glycerol, ethylene glycol (EG), and dimethyl sulfoxide (DMSO). Layer thickness, polymer volume fraction, and shear modulus of the polymer films with varying co-solvent concentration are determined with this approach. It was found that preferential hydrogen-bonding interactions of solvent mixtures with the polymers leads to variation in the structural properties of the polymer brushes upon changing the co-solvent composition. Furthermore, the conformation of polymer brushes in solvent mixtures is influenced by the solvent–solvent interactions, which can be explained in terms of the free energy of solvent mixing.



1. INTRODUCTION

The quartz crystal microbalance (QCM) is a mechanosensing device, developed to estimate the film thickness of rigid films deposited in air or vacuum. QCM detects small changes in added mass of the crystal by observing the change in the crystal's resonant frequency. AT-cut piezoelectric quartz crystals can operate in a thickness shear mode, in which an acoustic wave is generated with a frequency given by¹

$$f_n = \frac{n}{2d} \left(\frac{\mu_q}{\rho_q} \right)^{1/2} \quad (1)$$

where f_n is the resonant frequency of the quartz crystal, μ_q the shear modulus of the quartz, ρ_q the density of the crystal, d the plate thickness, and n the overtone number. The change in resonant frequency at a specific overtone ($\Delta f_{\text{mass},n}$) upon

deposition of rigid films onto the quartz surface is related, via the Sauerbrey equation,² to the adsorbed mass:

$$\Delta f_{\text{mass},n} = -\frac{f_n}{d\rho_q} \Delta m \quad (2)$$

where Δm is the surface mass density of the adlayer.

However, the change in the frequency of the quartz resonator at a determined overtone results not only from the contribution of rigid adlayer mass (Δf_{mass}) but also from several factors such as the viscosity of the liquid (Δf_η), surface topography of the crystal (i.e., the roughness, $\Delta f_{\text{roughness}}$), and the binding nature of the adlayer to the crystal (slip/no-slip, Δf_{slip})

Received: November 1, 2012

Revised: January 6, 2013

$$\Delta f = \Delta f_{\text{mass}} + \Delta f_{\eta} + \Delta f_{\text{roughness}} + \Delta f_{\text{slip}} \quad (3)$$

If the frequency shift is much smaller than the resonance frequency, as is the case in our measurements, the QCM response Δf can be described in the first-order approximation with respect to the film thickness. Within this approximation, the frequency terms collected in eq 3 are independent of each other and thus additive.³ The quartz crystal microbalance is also being increasingly used to determine the physical properties of macromolecular films, such as polymer brushes,^{4–6} adsorbed proteins,^{7,8} or self-assembled monolayers (SAM).⁹ These viscoelastic adlayers undergo considerable internal motion when oscillated with the quartz crystal, leading to significant dissipative losses with long relaxation times. Thus, to estimate mechanical properties of these structures with high accuracy, the dissipation response of the quartz resonator should also be taken into account. To this end, the AC driving waveform to the quartz crystal is cut off and the decay in the amplitude of oscillation is measured. In this way the dissipation energy (FWHM) of the quartz crystal due to the adlayer can be determined and is given as a dissipation parameter, ΔD . The value of this parameter incorporates effects due to both adlayer and associated solvent.

Several theoretical models, such as the electrical equivalent circuit (Butterworth–van Dyke circuit model^{11,10,11}), its extended analysis by Johannsmann^{12,13} (small-load approximation, or SLA), and continuum mechanical descriptions (Maxwell or Voigt model) have been proposed to describe the response of the acoustic resonator.¹⁴ The SLA relates the frequency shift with the load impedance of the adlayer, which gives the ratio between lateral stress to lateral speed at the acoustic interface. The Voinova model¹⁵ describes the interfacial response of polymer films using Voigt–Kelvin-based elements. The mechanical properties of the viscoelastic films are related to the stored energy and the dissipation processes resulting from the relaxation response of the polymer film to the shear stress applied by the resonator. Both Voigt and SLA approaches have been demonstrated to be *equivalent* for viscoelastic films in a liquid,¹³ extending the Sauerbrey equation with a correction for the viscoelastic response of the adlayer and allowing an estimation of the shear modulus of the films.

In our present study we introduce a new approach, the two-fluid model—a model previously used for polymers in bulk^{16–20}—which describes the effect of a two-phase film consisting of adsorbed copolymer (solid phase) and associated solvent mixture (liquid phase) on the QCM response, when operated in contact with semi-infinite liquids. Navier–Stokes–Brinkman and elastic wave equations are used to model the two-phase film adsorbed on the quartz crystal, with a Darcy term to account for the interactions between the two phases. This approach is more comprehensive than Voigt’s method, since it accurately describes the velocity profile in the film and allows several factors, such as slip length, monomer density in the film, and surface roughness, to be taken into account, which would not be possible by using Voigt’s approach. Johannsmann has extended the SLA approach to include slip at the crystal interface²¹ and has combined the SLA approach with FEM numerical simulations,²² which is more appropriate for the investigation of the dissipation mechanism for an adlayer of discrete (bio)molecular objects, such as proteins or adsorbed nanoparticles. This, however, is beyond the scope of the present study.

Properties of polymer-bearing surfaces can be effectively tuned by altering parameters such as molecular weight, grafting density, and solvent quality surrounding the polymer brush.²³ In order to have precise control over polymer properties, the use of solvent mixtures (i.e., varying the volume percentage of the co-solvent in aqueous solution) has been shown to be an effective approach.^{24,25} In this work, two polyelectrolyte copolymer brushes, poly(L-lysine)-*graft*-poly(ethylene glycol) (PLL-*g*-PEG) and poly(L-lysine)-*graft*-dextran (PLL-*g*-dextran), are studied in aqueous mixtures of glycerol, ethylene glycol, and DMSO. Water-soluble PEG is insoluble in glycerol and ethylene glycol, whereas dextran interacts with all three solvents and with water via hydrogen bonding. These mixed solvents thus exhibit a variety of solvent qualities for the PEG/dextran brushes in comparison to those of the pure aqueous buffer. The response of the adsorbed polymer brushes to different solvent qualities is studied using a quartz crystal microbalance, and the two-fluid model is applied to estimate quantitatively the resulting collapse or stretching of the polymer brushes upon varying solvent quality.

2. TWO-FLUID MODEL

The two-fluid model describes the effect of the two phases in the film: the adsorbed polymer (elastic solid phase) and the associated solvent mixture (viscous liquid phase), on the QCM response, when operated in contact with a semi-infinite fluid medium (Figure 1). Navier–Stokes–Brinkman and elastic wave

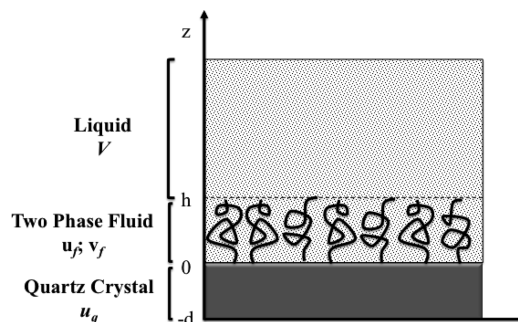


Figure 1. Schematic representation of interfacial geometry of the polymer film on a quartz crystal substrate. The z -axis is perpendicular to the quartz interface.

equations with the Darcy terms describe the coupled motion of the liquid and the polymer in the film that is adsorbed on the quartz crystal. This approach makes it possible to account for the differences in the slip behavior of each phase at the QCM surface and at the film–bulk liquid interface, by considering the relevant boundary conditions for each phase.

The Navier–Stokes–Brinkman equation for the liquid phase (eq 4) and the elastic wave equation for the polymer (solid) phase (eq 5) under oscillatory movement are given by

$$i\omega\rho_l V_f(z) = \eta \frac{d^2 V_f(z)}{dz^2} + \eta \xi^{-2} (i\omega u_f(z) - V_f(z)) \quad (4)$$

$$-\omega^2 \rho_s u_f(z) = K \frac{d^2 u_f(z)}{dz^2} - \eta \xi^{-2} (i\omega u_f(z) - V_f(z)) \quad (5)$$

where $V_f(z)$ and $u_f(z)$ are the velocity of the liquid and the displacement of the polymer in the film, respectively, η is the fluid viscosity of the film, K is the shear modulus of the solid phase, and ρ_l and ρ_s are weighted densities of liquid and solid

phases with $\rho_l = (1 - \phi)\rho_0$ and $\rho_s = \phi\rho_p$, ϕ being the volume fraction of the polymer in the film. ρ_0 and ρ_p are the densities of the solvent mixture and of the dry polymer, respectively.

The drag force that results from the flow of the liquid through the porous polymer is described by a Darcy-type term in eqs 4 and 5 (second term on the right-hand side of both equations). This force is a function of the relative velocities of polymer and liquid, of the liquid viscosity, and of a parameter called the hydrodynamic screening length (ξ). The physical meaning of ξ depends on the nature of the interfacial layer. For instance, for rough surfaces, ξ is related to the porosity of the interfacial layer and for a polymer layer ξ corresponds to the correlation length.^{26,27}

Equations 4 and 5 can be rewritten as

$$\frac{d^2 V_f(z)}{dz^2} = q_1^2 V_f(z) - i\omega\xi^{-2} u_f(z) \quad (6)$$

$$\frac{d^2 u_f(z)}{dz^2} = p_1^2 u_f(z) - \frac{\eta\xi^{-2}}{K} V_f(z) \quad (7)$$

where

$$q_1^2 = q_{01}^2 + \xi^{-2}, \quad q_{01}^2 = \frac{i\omega\rho_l}{\eta}$$

$$p_1^2 = -p_0^2 + \frac{i\omega\eta}{K}\xi^{-2}, \quad p_0^2 = \frac{\omega^2\rho_s}{K}$$

The solutions for eqs 6 and 7 have the following form:

$$V_f(z) = \sum_{j=1}^4 C_j \exp(\lambda_j z) \quad (8)$$

$$u_f(z) = \sum_{j=1}^4 C_j \alpha_j \exp(\lambda_j z) \quad (9)$$

The expressions for the coefficients C_j , α_j , and λ_j for $j = 1-4$ are given in the Supporting Information. The coefficients α_j and λ_j are determined by properties of the film, while C_j depends on the considered boundary conditions.

In the QCM experiments, the polymer film of thickness h is adsorbed from the buffer solution and the two-phase film is considered to have homogeneous lateral density on the quartz crystal. The z -axis is considered to be perpendicular to the quartz surface and the plane $z = -d$ coincides with the constrained face of the quartz resonator, where d is the thickness of the quartz crystal. The unconstrained interface of the quartz crystal at $z = 0$ has an oscillatory motion, which generates a shear wave in the film and in the bulk liquid above the adlayer (Figure 1). The shear oscillations in the quartz crystal u_q and the velocity of the bulk fluid V are given by

$$u_q(z) = A \cos(k_q(z + d)) / \cos(k_q d), \quad -d < z < 0 \quad (10)$$

$$V(z) = V(h) \exp(-q_0(z - h)), \quad z > h \quad (11)$$

where $k_q = \omega(\rho_q/\mu_q)^{1/2}$ is the wavenumber of the shear wave of the quartz, $q_0^2 = i\omega\rho_0/\eta_0$, where ρ_0 and η_0 are density and viscosity of the bulk fluid, A is the amplitude of the displacement of the interface (at $z = 0$), and the velocity of the interface is given by $V_0 = i\omega A$.

The following boundary conditions are considered for the system:

$$V_f(0) = V_0 \quad (12)$$

$$i\omega u_f(0) = V_0 \quad (13)$$

$$V_f(h) = V(h) \quad (14)$$

$$\lambda \frac{dV_f(h)}{dz} = V(h) - i\omega u_f(h) \quad (15)$$

$$\eta_0 V(h) \frac{dV_f(h)}{dz} - Ki\omega u_f(h) \frac{du_f(h)}{dz} - \eta V(h) \frac{dV_f(h)}{dz} = 0 \quad (16)$$

Equations 12 and 13 consider that at the quartz–film interface ($z = 0$) the velocities of both phases in the film are equal to the velocity of the quartz (V_0). At $z = h$ the velocity of the liquid phase in the film is equal to the velocity of the bulk liquid $V(h)$ (eq 14). Equation 15 considers the possibility of slip between the polymer phase and the bulk liquid at the interface $z = h$ with a slip length of λ . Equation 16 represents the continuity of the density of energy flux at the interface $z = h$. The above boundary conditions are applied to calculate values of C_j , which define the velocity of the liquid and the displacement of the polymer ($V_f(z)$ and $u_f(z)$). The general expressions for the coefficients C_j for $j = 1, \dots, 4$, for a zero slip length, are given in the Supporting Information.

The complex frequency shift ΔF (where F is related to the angular frequency ω by $\omega = 2\pi F$) consists of real and imaginary components, which are given by the resonant frequency shift Δf and the dissipation shift $\Delta\Gamma$, respectively, both obtained experimentally from QCM-D. To correlate the complex resonant frequency shift with the film properties, the balance of forces per unit area at the interface $z = 0$ is considered:

$$\mu_q \frac{du_q(0)}{dz} - n \frac{dV_f(0)}{dz} - K \frac{du_f(0)}{dz} = 0 \quad (17)$$

The solution of eq 17 is the complex frequency shift ΔF

$$\Delta F = -\frac{if_n}{n\pi\sqrt{\rho_q\mu_q}} \frac{1}{V_0} \left[\eta \frac{dV_f(0)}{dz} + K \frac{du_f(0)}{dz} \right]$$

Or in another form, substituting eqs 8 and 9:

$$\Delta F = \frac{2f_n^2 \rho_0 \eta}{n\pi q_0^2 \eta_0 \sqrt{\rho_q \mu_q}} \frac{1}{V_0} \left[\sum_{j=1}^4 \lambda_j C_j + \frac{K}{i\omega_n \eta} \sum_{j=1}^4 \lambda_j \beta_j C_j \right] = \Delta f + i\Delta\Gamma \quad (18)$$

Here $\beta_j = i\omega\alpha_j$ and $q_0^2 = i\omega\rho_0/\eta_0$. Hence, the experimentally determined parameters Δf and $\Delta\Gamma$ are a function of the coefficients C_j , λ_j , and β_j . It should be noted that $\Delta\Gamma$ is related to the measured dissipation change ΔD as $\Delta\Gamma = (\Delta D f_n)/2$. Thus, the coupled system of equations can be solved with the experimentally determined Δf and $\Delta\Gamma$ to determine the physical properties of the system, such as the shear modulus of the polymer (K), the hydrodynamic screening length (ξ), the density of the solid phase (ρ_s), the thickness of the film (h), and the slip length (λ).

In the case of thin films, $|\lambda_j h| \ll 1$ for $j = 1-4$ and $|q_0 h| \ll 1$, and zero slippage at all interfaces the two-fluid model reduces to the Voigt model,^{12,15} where the density of the polymer film

is given by the average density ($\rho_{\text{avg}} = \rho_s + \rho_l$). In this case the complex frequency shift is given by

$$\Delta F_{\text{voigt}} = -\frac{if_n}{\pi\sqrt{\rho_q\mu_q}} \left[-q_0\eta_0 - i\omega\rho_{\text{avg}} \left(1 - \frac{i\omega\rho_0\eta_0}{(K + i\omega\eta)\rho_{\text{avg}}} \right) \right] \quad (19)$$

3. MATERIALS AND METHODS

3.1. Materials. Polyelectrolyte copolymers PLL(20 kDa)-g[3.6]-PEG(5 kDa) and PLL(20 kDa)-g[3.5]-dextran(5 kDa) were purchased from SuSoS AG (Dübendorf, Switzerland) with molecular weights of the PLL backbone of 20 kDa and of the side chains (PEG/Dextran) of 5 kDa. A grafting ratio (defined as number of lysine units/total number of amine groups in the backbone) close to 3.5 was used for both the copolymers. HEPES (10 mM of 4-(2-hydroxyethyl)-1-piperazine-1-ethanesulfonic acid (Sigma, St. Louis, MO), adjusted with 6.0 M NaOH solution) was used as the aqueous buffer to maintain the pH at 7.4. The PLL-g-PEG and PLL-g-dextran copolymers in aqueous buffer with a concentration of 0.25 mg/mL were adsorbed onto silica surfaces. The charged poly(L-lysine) backbone adsorbs on silica via electrostatic interactions to form moderately dense PEG or dextran brushes in pure HEPES. Solvent mixtures of HEPES with glycerol (ABCR GmbH, Karlsruhe, Germany), ethylene glycol (Sigma-Aldrich), or DMSO (Alfa Aesar, Karlsruhe, Germany) were prepared (all defined as volume percentages). All solvent mixtures were freshly prepared before the start of the experiment, and their densities and viscosities are given in the Supporting Information. The dry densities of poly(ethylene glycol) and dextran polymers are considered as being approximately 1.08 and 1.4 g/cm³, respectively.

3.2. Transmission Interferometry Adsorption Sensor (TInAS). The transmission interferometric adsorption sensor (TInAS, a home-built device) is a label-free sensing instrument.²⁸ The adsorption sensor is a stacked, transparent multilayer structure. The layers, which have different refractive indices, consist of a spacer layer (silica with a thickness ≈ 2.5 μm), a mirror (aluminum coating with thickness ≈ 20 nm), and a glass substrate. When white light is passed through the sensor, the transmitted interference pattern, which consists of secondary fringes caused by partial reflections at each optical interface, is collected by an optical spectrometer. The shift in the interference pattern (secondary fringes) upon adsorption of polymer films provides a measurement of the film thickness of the adlayer. The fast spectral correlation (FSC) method²⁹ gives the thickness of the adlayer in real time with a resolution of ± 25 pm. Also, the refractive index of the adlayer can be simultaneously determined, according to a recently developed numerical algorithm.³⁰

A closed sample cell, with an ability to exchange liquids, enables the study of the adsorption kinetics of polymers onto a surface. In this study, SiO₂ was used as spacer layer and also as substrate for the polymer adsorption. The resulting effective optical thickness D is transformed into dry adsorbed mass (per unit area) of the polymer according to

$$M = \rho_p D = \frac{n_A - n_C}{dn/dc} D \quad (20)$$

where ρ_p is the dry density of the polymer, which is a function of the refractive index difference between the adsorbate (n_A) and the solvent (n_C) and is normalized by the concentration dependence of the refractive index in the mixture of polymer and solvent (dn/dc). In this study, the value for dn/dc for PLL-g-PEG and PLL-g-dextran in aqueous medium was considered as 0.139 cm³ g⁻¹, and the refractive indices for polymer and HEPES were assumed to be 1.45 and 1.33, respectively.³¹ Sensors were incubated in HEPES buffer overnight to attain stable baselines before the adsorption measurement.

3.3. Quartz Crystal Microbalance. AT-cut quartz crystals (diameter = 25 mm) coated with SiO₂ (QXS 303, LOT Oriel Group, Germany) with a fundamental frequency of 4.95 MHz were used to study the structural transitions of the adsorbed polymer upon variation of the composition of the aqueous solvent mixtures. Changes in frequency Δf and dissipation ΔD of the crystal resonator (Q-Sense, Sweden) were measured over different overtones ($n = 3$ to $n = 11$). Quartz crystals were sonicated in ethanol for 30 min and then ozone treated for 30 min before placing them in the QCM chamber. Inlet and outlet tubing and the QCM chambers were rinsed with ultrapure water (GenPure UV, TKA GmbH, Niederelbert, Germany) before use. The fundamental frequencies were characterized in ultrapure water. The chamber is designed to provide a nonperturbing exchange of liquids over the quartz crystal by means of a pump. A flow rate of 20 $\mu\text{L}/\text{min}$ was used, and the chamber temperature was maintained at 25 $^{\circ}\text{C}$ during all measurements.

4. RESULTS

4.1. Estimation of Dry Mass of Adsorbed Polymer. The adsorption kinetics and dry mass adsorbed at equilibrium were measured for the two selected polymers on a silica surface by means of TInAS. All experiments were conducted at room temperature. Figure 2 shows the adsorption kinetics for PLL-g-

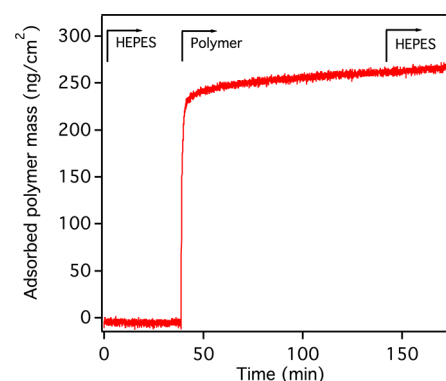


Figure 2. Adsorption kinetics of PLL-g-PEG from HEPES, at a concentration of 0.25 mg/mL, onto a SiO₂-coated TInAS sensor. The order in which solutions are injected into the TInAS cell are indicated by horizontal arrows.

PEG from aqueous buffer (10 mM HEPES) onto a SiO₂-coated substrate. Once a stable baseline was achieved, in buffer, the copolymer, with a concentration of 0.25 mg/mL in buffer, was injected into the cell. The adsorption of the polymer was carried out for 90 min, after which the cell was rinsed with buffer to remove physically adsorbed polymer from the surface of the sensor. However, no significant loss in the polymer was observed during rinsing. The difference in dry mass after rinsing

the polymer film with HEPES and the obtained baseline in the buffer gives the adsorbed dry mass of the polymer film. The adsorbed mass of PLL-g-PEG and PLL-g-dextran on a silica surface, as estimated from eq 20, is found to be 268 ± 14 and 288 ± 10 ng/cm², respectively.

4.2. QCM Studies of Polymer Brushes. To correctly interpret the QCM response of the adsorbed polymer films, it is important to identify the possible influence of the SiO₂ substrate on length scales relevant to QCM studies. For a flat surface in the absence of polymer, the change in frequency and dissipation when normalized by the density of the solvent (ρ_0) and the overtone number (n) is a linear function of the velocity decay length ($\delta_n = (\eta_0/\pi n f \rho_0)^{1/2}$) of the shear wave in the corresponding medium. Any deviation of frequency and dissipation from this response indicates the effect of roughness^{32–34} or chemical change at the interface.³⁵ Our results (see the Supporting Information) demonstrate that the SiO₂ surface is flat on the scale of several hundreds of nanometers (also confirmed by AFM) and remains chemically unmodified. Hence, the QCM response of the adsorbed polymers is not affected by any substrate effect.

Figure 3 shows representative QCM results for the change in frequency, normalized by the overtone (in Hz), and for the

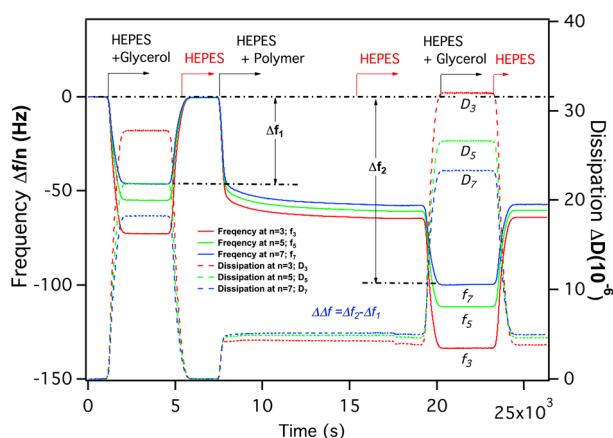


Figure 3. Normalized frequency $\Delta f/n$ (solid lines) and dissipation ΔD (dotted lines) at three different overtones ($n = 3, 5$, and 7) obtained for PEG brushes in HEPES–10 vol % glycerol. The order in which solutions are injected into the QCM cell are indicated by horizontal arrows. In the figure, Δf_1 represents the frequency change due to the viscosity of solvent mixture and Δf_2 represents the frequency change due to the adsorbed polymer mass, associated solvent mixture, and the viscosity effect of the solvent mixture. The effect of polymer adsorption in a given solvent mixtures is thus given by $\Delta \Delta f = \Delta f_2 - \Delta f_1$.

dissipation as a function of time for a PEG brush in a solvent mixture of HEPES and 10 vol % glycerol at three different overtones (third, fifth, and seventh harmonic). The differences in frequency shifts for different overtones are due to the viscous nature of the solvent mixtures and the viscoelastic nature of the polymer films (Figure 3).

The baseline for the quartz crystal was obtained with aqueous buffer (HEPES). To determine the changes in conformational properties of polymer film in viscous solvent mixtures, the effect of the viscosity of the solvent mixture on the response of the quartz crystal must be considered.³⁶ Thus, the buffer solution was exchanged with the solvent mixture (here HEPES + 10 vol % glycerol) prior to polymer adsorption,

and the changes in frequency and dissipation due to the viscous forces from the solvent under shear were obtained. This “viscosity effect” is represented as Δf_1 in Figure 3. The solvent mixture was then exchanged back to HEPES, and the baseline was regained. PLL-g-PEG polymer dissolved in HEPES (0.25 mg/mL) was injected into the cell, and the adsorption was carried out for ~ 45 min. The aqueous buffer was then injected into the cell to remove the loosely bound polymers from the quartz surface. Finally, the HEPES was exchanged with the corresponding solvent mixture (HEPES + 10 vol % glycerol), resulting in a total frequency change, Δf_2 . Thus, the effect of polymer adsorption ($\Delta \Delta f$) in a given solvent mixture is determined by subtracting the viscosity effect from Δf_2 , i.e., $\Delta f_2 - \Delta f_1$ (see the Supporting Information). The effect of polymer adsorption includes the contribution of both the inertial mass of the polymer and of the solvent mixture, which cannot be separated in the total QCM response, since adsorption was performed from the HEPES buffer solution in all experiments, in order to achieve the same grafting density of the polymer. To check the absence of desorption of the polymer during solvent exchange, HEPES solution was injected back into the cell at the end of the experiment, and it was determined that the frequency and dissipation values prior to the solvent exchange were regained. A similar protocol was used for PEG and dextran brushes in aqueous mixtures of glycerol/EG/DMSO at different volume percentages of the co-solvent, in order to estimate Δf_1 and Δf_2 . Figure 4 shows the changes in frequency

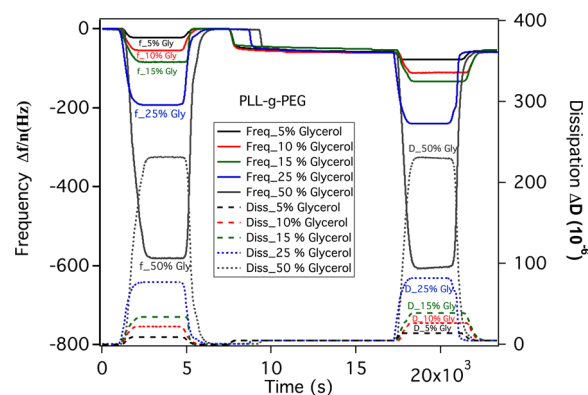


Figure 4. QCM response indicating the changes in frequency (solid lines) and dissipation (dotted lines) with time obtained for PEG brushes in aqueous glycerol mixtures of different compositions (5, 10, 15, 25, and 50 vol % of glycerol in aqueous buffer) for the fifth overtone.

and dissipation response at the fifth overtone obtained for PEG brushes with increasing glycerol percentage in the solvent mixture. The frequency change due to the viscosity effect (Δf_1) increases with increasing glycerol volume fraction in the solution due to the increased viscosity of the bulk solution.

Figure 5 represents the change in frequency shift ($\Delta \Delta f$) for PEG and dextran brushes in aqueous solvent mixtures of glycerol, EG, and DMSO for the ninth overtone. High overtones (such as $n = 9$) are employed for the analysis, since the corresponding frequencies have a shorter decay length from the crystal surface and thus can probe the film properties most effectively. Since no desorption of the polymer occurs upon solvent exchange, the changes in the frequency shift can be related to the amount of associated solvent that is gained or lost by either stretching or collapse of the polymer film,

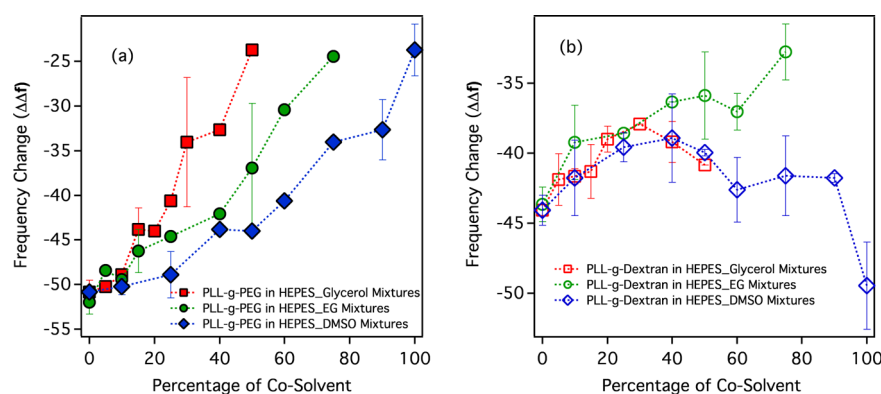


Figure 5. Changes in frequency shift ($\Delta\Delta f = \Delta f_2 - \Delta f_1$), for the ninth overtone, due to conformational transitions of (a) PEG and (b) dextran brushes with change in co-solvent percentage in glycerol, EG, and DMSO aqueous mixtures as obtained from QCM measurements.

respectively, due to a conformational change as a function of co-solvent percentage. The PEG brushes in all the studied solvent mixtures show larger collapse in comparison to the dextran brushes.

Figure 6 shows the corresponding changes in dissipation. Dextran chains being shorter and stiffer than PEG (the

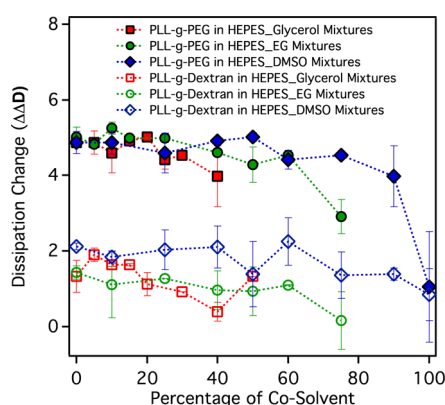


Figure 6. Changes in dissipation, for the ninth overtone, with respect to percentage of co-solvent in aqueous mixtures of glycerol/EG/DMSO for both PEG (closed symbols) and dextran brushes (open symbols), as obtained from QCM measurements.

repeating unit of dextran polymer has a greater length, which leads to a higher persistence length) lead to lower dissipation. The changes in dissipation for polymer brushes with increase in

co-solvent percentage are not as pronounced as the obtained changes in frequencies.

4.3. Modeling of the QCM Data with “Two-Fluid Model”. The frequency and dissipation responses of the polymer film in different solvent mixtures, obtained from QCM experiments, were used as input data for the two-fluid model, in order to estimate physical properties of the adsorbed polymer brushes. The slip between the polymer film and the unconstrained interface of the crystal is negligible due to the strong electrostatic interaction of polymer backbone with the surface. Also, a negligible slip between the polymer and the bulk fluid medium seems reasonable to assume for hydrophilic polymers (PEG and dextran) in aqueous mixed solvents. Even PEG and dextran brushes in poor solvents, such as 100 vol % glycerol and EG, can be assumed to have a negligible slip as the brushes only have moderate packing density at the interface.

Figure 7 gives the film thickness of the PEG and dextran brushes with change in co-solvent percentage (θ) in the solvent mixtures, obtained with the two-fluid model. PEG brushes in pure aqueous buffer have a higher film thickness than those observed for dextran brushes. This is to be expected, since although the repeat unit of the ethylene glycol (0.35 nm)³⁷ is smaller than that of dextran (0.7 nm)³⁸, the degree of polymerization (N) is 109.9 and 31.8 for PEG and dextran chains, respectively.

PEG brushes show a collapse (i.e., decreasing film thickness at constant adsorbed mass) for all the three solvent mixtures with increase in co-solvent percentage. The collapse of PEG films with respect to solvent composition is very similar in all

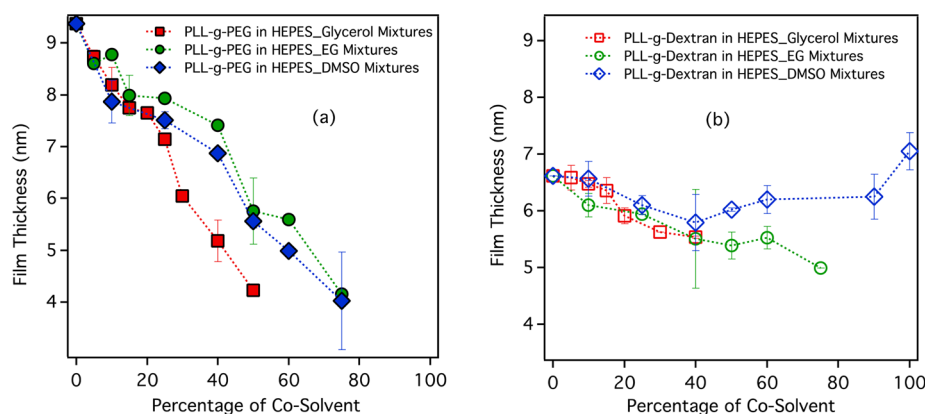


Figure 7. Film thicknesses of PEG (a) and dextran (b) brushes as a function of co-solvent percentage obtained with the two-fluid model.

the studied solvent mixtures (Figure 7a). At concentrations above 75 vol %, significant scatter in the measurements of dissipation is observed, probably due to viscosity of the solvent. The two-fluid model description of the film-thickness measurements indicates that PEG brushes are poorly solvated by the three selected co-solvents in comparison to water. If the volume percentage of co-solvent in aqueous solution is increased to 50%, PEG brushes show a collapse of about 45% from their original height ($h(\theta=50)/h(\text{HEPES})$). For the same increase of co-solvent volume fraction in the mixture, dextran brushes show a smaller collapse for all solvents mixtures (Figure 7b). Dextran brushes in aqueous DMSO mixtures show an initial collapse in film thickness below a DMSO volume fraction of 50%. At higher DMSO percentages (>50%), a stretching of the polymer brush is observed (Figure 7b). This anomalous behavior of dextran brushes in aqueous mixtures of DMSO can be explained via preferential solvation of the polymer by two competing good solvents (water and DMSO) that are also significantly interacting with each other.^{39–41} This will be discussed later. The film thicknesses obtained from the two-fluid model were compared with results from Voigt's model (eq 19), and the difference in the calculated film thickness using both the models was found to be negligible.

Applying the principle of conservation of mass for the polymer phase in the two-phase film, in its stretched or collapsed form, it is possible to estimate the volume fraction of the polymer in different solvent mixtures with the obtained film thickness (h) as

$$\phi = \frac{1}{1 + h(1 - \phi_{\text{HEPES}})/(\phi_{\text{HEPES}}h_{\text{HEPES}})} \quad (21)$$

where ϕ_{HEPES} and h_{HEPES} are the volume fraction and the thickness, respectively, of the polymer film in pure HEPES solution. The collapse of the polymer film, i.e., the decrease in film thickness with decrease in solvent quality, leads to an increase of the volume fraction of polymer and the expulsion of the solvent from the two-phase system, while stretching has the opposite effect. The density of the polymer film can thus be estimated as $\rho_{\text{avg}} = \rho_p\phi + \rho_o(1 - \phi)$ (where $\phi = \phi$, when no phase separation of the solvent mixtures within and outside the polymer film is considered), and the net areal solvation of the polymer brushes (Ψ) is calculated, which is an important parameter to determine antifouling⁴² or lubrication³⁶ properties of polymer brushes. The net areal solvation can be defined as the amount of solvent that participates in the solvation of the brush in a given unit area and is estimated by subtracting the dry mass of polymer film (m_{dry} as estimated from TInAS) from the wet polymer film mass ($m_{\text{wet}} = \rho_{\text{avg}}h$, as estimated with the two-fluid model). The estimated areal solvation for PEG and dextran brushes in different solvent mixtures is shown in Figure 8. Higher areal solvation is measured for PEG brushes in comparison to dextran brushes. Also, the number of solvent molecules per monomer can be estimated from the experimentally obtained values of m_{dry} and m_{wet} and can be described as $\Lambda_{\text{sol/monomer}}$ (from eqs 2–4 in ref 36). The average ratios of monomers to solvent molecules measured for PLL-g-PEG ($\Lambda_{\text{sol/EG}}$) and PLL-g-dextran ($\Lambda_{\text{sol/dextran}}$) in pure aqueous solution were estimated as 7 and 14, respectively, showing that both brushes are well hydrated in aqueous buffer. The solvent molecules per monomer for solvent mixtures cannot be estimated by the above-mentioned equations due to possible preferential solvation and demixing between the two co-

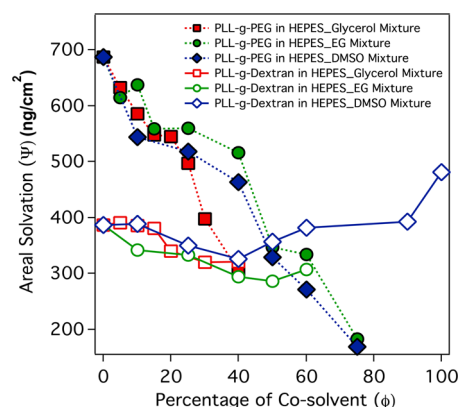


Figure 8. Areal solvation (Ψ) for PEG and dextran brushes as a function of co-solvent percentage calculated by subtracting the wet mass of the polymer film (solvent + polymer mass) obtained from the two-fluid model with the dry mass of polymer film (polymer mass only) obtained from TInAS.

solvents of the co-solvent with the monomer. However, PEG brushes show a steep decrease in areal solvation in comparison to dextran brushes upon increasing co-solvent percentage.

Lastly, the two-fluid model is used to estimate the shear modulus of the polymer film in solvent mixtures with varying solvent quality. According to eq 18, the shear modulus of thin polymer films, of thickness smaller than the velocity decay length, is inversely related to the measured dissipation response. Hence, the accuracy of determination of the shear modulus is related to the accuracy of measurement of the dissipation. The factors that contribute to the dissipation response are the flow of the solvent passing through the polymer chains, which leads to viscous drag forces, viscous dissipation in the bulk liquid, and the mechanical properties (elastic behavior) of the adsorbed polymer. The dissipation factor ΔD (as measured by QCM) is a result of these combined contributions, and according to the two-fluid model (eq 18), the shear modulus can be determined from the measured dissipation factor ΔD (or $\Delta\Gamma$). Figure 9 shows the shear modulus of the polymer films in aqueous mixtures of glycerol/EG/DMSO as a function of co-solvent percentage. An increase in shear moduli for PEG and dextran brushes is seen with increase in co-solvent percentage in the solvent mixture. Despite the more facile solvation of dextran brushes in comparison to PEG brushes, the shear moduli of the dextran brushes are higher than those of the PEG brushes. The high persistence length of the dextran monomer as well as the shorter chain lengths of dextran (5 kDa) results in stiffer films, in comparison to those of PEG (5 kDa). Shear moduli may affect the frictional response of polymer brushes, as will be discussed in a future communication.

5. DISCUSSION

The equilibrium conformation of the polymer chain adsorbed on the surface is governed by two energetic terms: the excluded-volume term, which results from the interaction forces between adjacent polymers and between the polymer and solvent, and the restoring elastic term, which results from tethering the polymer chain to the substrate. Polymer brushes have been shown to stretch in good solvents, in order to maximize the polymer–solvent interactions, and to collapse upon decreasing solvent quality. However, in the case of solvent mixtures, not only the polymer–solvent pair interactions but

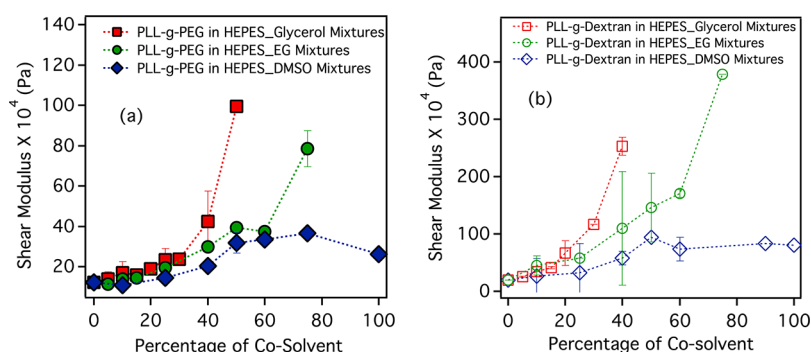


Figure 9. Shear modulus of the polymer films as a function of co-solvent percentage in aqueous solution as obtained from the two-fluid model for (a) PEG and (b) dextran brushes.

also the solvent–solvent interaction energy has to be considered, in order to estimate the structural properties of the polymer brushes.

Aqueous solutions of glycerol, ethylene glycol, and DMSO are widely used as cryosolvents to preserve proteins and other biomolecules.⁴³ These co-solvents are highly polar and have a tendency to form hydrogen bonds not only with hydrophilic polymers (except for PEG in glycerol and EG solutions) but also with each other. The solvation effect on the conformation of hydrophilic polymers such as PEG and dextran in bulk solvent mixtures has been studied in the literature via diverse thermodynamic approaches,⁴⁴ which differ in their predictions. For example, solubility can be estimated through the interfacial free energy, which gives the free energy of cohesion between polymer and solvent. Table 1 shows the interfacial free energy

Table 1. Calculated Interfacial Free Energies for PEG and Dextran Polymers, with Molecular Weights Similar to Those Used in Our Work, in Pure Solvents^a

ΔG (mJ/m ²)	water	glycerol	EG	DMSO
PEG (6 kDa)	43.623	−1.210	0.531	4.432
dextran (150 kDa)	40.725	−2.112	0.706	4.513

^aThe values are obtained from the literature.⁴⁵

for PEG and dextran polymers with molecular weights similar to those used in our studies, in glycerol, EG, and DMSO, calculated according to van Oss theory.⁴⁵ Positive values of ΔG indicate that the polymer dissolves in the solvent spontaneously while the polymer tends to precipitate for negative values of ΔG . According to Table 1, both PEG and dextran polymers are expected to dissolve in EG and DMSO mixtures and are not soluble in glycerol. ΔG values show high solubility of PEG and dextran in the pure aqueous solutions. Contrasting solubility trends for the same polymers in the selected solutions have been obtained through intrinsic viscosity measurements,^{24,46,47} which demonstrate the limitations of the current available thermodynamic models for predicting polymer solubility, especially for polar solvent–polymer interactions.

Solvation of polymer brushes does not seem to correlate with the solubility of the polymers in bulk solution, as given in Table 1, or with intrinsic viscosity measurements.^{24,46,47} Tethering the polymer to the surface drastically reduces the conformational freedom of the polymer, while solubility calculations for polymers in bulk solutions do not include the elasticity entropy term in the free energy. Such discrepancies between the properties of polymers in bulk and as a brush are observed for other systems.⁴⁸ Therefore, the most appropriate description of

the solvent quality for the polymer brush appears to be that obtained directly from the QCM structural measurements (stretching or collapse): PEG brushes collapse significantly in all investigated solvent mixtures due to a decrease in solvent quality. Although dextran brushes are better solvated in glycerol or EG solutions in comparison to PEG brushes, they still show a significant collapse. Only aqueous mixtures of DMSO solvate the dextran brushes as well as does pure water.

In a mixture of a good and a bad solvent, the good solvent preferentially participates in forming the solvation shell. Our studies show a linear decrease in polymer thickness with increasing concentration of poor/marginal solvent components in the solvent mixture, except in the case of dextran in aqueous–DMSO mixtures, where both components are good solvents for the polymer brush. Besides preferential solvation effects, the inherent solvent–solvent interactions play a significant role in the stretching/collapse behavior of the brush. If the interaction between the solvents is weak, as it is for 2-propanol and water⁴⁹ and also as estimated in Lai et al.,⁵⁰ preferential adsorption is further favored by the energetically favorable tendency of the bulk solution to demix: although the demixing between the two co-solvents implies an entropic penalty, it is favored by the stronger enthalpic increase due to the good solvation of PEG brushes by water. The PEG brushes in aqueous 2-propanol solution show a collapse only above a 2-propanol concentration of 85 vol %.⁴⁹ Below this concentration, the amount of solvent (water) in the brush remains approximately constant, as determined by QCM measurements.⁵¹

Preferential solvation in binary mixtures of solvents, obtained via a thermodynamic approach,⁵² estimates the self-interaction of the organic solvents when present in dilute aqueous solution. The self-interaction of the co-solvent is found to be higher for 2-propanol⁵³ in comparison to glycerol,⁵⁴ as the glycerol shows strong hydrogen-bonding tendencies toward water. Thus, the mixing enthalpy of water–glycerol/EG molecules is much higher in comparison to water–2-propanol; leading to demixing of water and glycerol/EG being energetically favorable (see mixing enthalpy of the mentioned solvent mixtures in the Supporting Information). As a consequence, both solvents, water and glycerol/EG, are present in the brush, which leads to brush collapse, even at low concentrations, thereby minimizing polymer–co-solvent interactions. This continuous collapse of PEG brushes in mixtures of water–glycerol at volume fractions of glycerol $\leq 50\%$ was also observed by means of the surface forces apparatus (see Supporting Information, in which the equilibrium brush lengths of polymer

brushes in aqueous solvent mixtures obtained from two different experimental approaches, QCM and surface force apparatus, are also compared).

Mixed solvents are often used to attain intermediate solvent quality, but sometimes the stronger interaction between the solvents than between solvents and polymer leads to a co-nonsolvency effect,⁵⁵ which causes collapse of the polymer brush at a critical co-solvent concentration. Dextran brushes in aqueous dimethyl sulfoxide mixtures show a decrease in film thickness with increasing DMSO concentrations up to 50 vol % of DMSO, after which the brush starts to stretch as the DMSO concentration is increased further. This behavior is also observed in our previous studies,⁴¹ where the film thickness and compressibility of the dextran brushes were determined using the surface forces apparatus. Both water and DMSO, being good solvents for polymer brushes, compete for solvation of the dextran film. However, at a critical concentration of co-solvent ($\theta \approx 50$ vol %) the interaction between dextran and the solvent mixture decreases due to maximum interaction energy between water–DMSO mixtures. The mixture behaves as a poor solvent, leading to a slight decrease in the film thickness. At higher concentrations of DMSO, the solvation of dextran is dominated by DMSO molecules and, since DMSO is a better solvent than water, results in a greater swelling of brushes in comparison to the situation in water.

Thus, the brush configuration, in equilibrium, results from the interplay between solvent quality, preferential solvation, and solvent–solvent interactions. By appropriate selection of solvent mixtures, the conformation of surface-adsorbed polymers, and hence both surface interactions and lubrication properties at the interface, can be tuned.

6. CONCLUSIONS

The two-fluid model has been applied to quantify the QCM-D response of polymer brushes in liquid media. This model uses the Navier–Stokes–Brinkmann equation to describe the motion of two phases (polymer and the solvent) in the film, when oscillated by quartz crystal, to estimate physical properties of PEG and dextran brushes, such as film thickness, volume fraction, and shear modulus, as a function of solvent composition. The model also allows slip and substrate roughness to be taken into account. The thickness of the polymer films in the solvent mixtures calculated by the two-fluid model from our experiments (no slip and slight roughness) is in good agreement with the results of conventional QCM models. PEG brushes show a higher degree of collapse in the selected solvent mixtures in comparison to dextran brushes, indicating the poor solvent quality of the mixtures for the PEG brushes. Dextran brushes exhibit higher shear moduli than PEG brushes, despite being better solvated, due to the higher stiffness of the dextran chains. Differences in the solvation behavior between polymers in bulk solution and polymer brushes (characterized by a collapse or stretching) have been identified and assigned to the difference in entropy elasticity of the polymer in bulk and when tethered to the surface. The stretching/collapse behavior of the polymer brushes results from the interactions between polymer and both co-solvents and as well from the interaction strength between the two co-solvents, as shown for the studied polymer brushes in aqueous mixtures.

■ ASSOCIATED CONTENT

■ Supporting Information

A detailed description of the solutions of equations from the two-fluid model, results of the study on the influence of surface topography of the quartz crystal on the QCM response before the adsorption of polymers, comparing film thickness of PEG films in aqueous–glycerol mixtures and dextran films in aqueous–DMSO mixtures as measured using the surface forces apparatus and the quartz crystal microbalance, the mixing enthalpies of solvent mixtures as a function of mole fraction of the co-solvent in the solution, and the viscosity and densities values of aqueous solutions of glycerol, ethylene glycol, and DMSO considered in this study is given. This material is available free of charge via the Internet at <http://pubs.acs.org>.

■ AUTHOR INFORMATION

Corresponding Author

*Phone +41-44-632-5850; e-mail nspencer@ethz.ch.

Present Address

^{||}Department of Mechanical Engineering and Applied Mechanics, University of Pennsylvania, Philadelphia, PA 19104.

Author Contributions

[§]Authors with equal contribution to the work.

Notes

The authors declare no competing financial interest.

■ ACKNOWLEDGMENTS

The financial assistance of the European Science Foundation, through their Eurocores (FANAS) program is gratefully acknowledged. We thank Alireza Mashaghi from the biophysics group, AMOLF Institute, Netherlands, for fruitful discussions and his valuable suggestions in this project.

■ REFERENCES

- (1) Steinem, C.; Janshoff, A. *Piezoelectric Sensors*; Springer-Verlag: Berlin, 2007.
- (2) Sauerbrey, G. Verwendung Von Schwingquarzen Zur Wagung Dunner Schichten Und Zur Mikrowagung. *Z. Phys.* **1959**, *155*, 206–222.
- (3) Urbakh, M.; Tsionsky, V.; Gileadi, E.; Daikhin, L. *Piezoelectric Sensors*; Springer-Verlag: Berlin, 2007; pp 111–149.
- (4) Zhang, G. Z.; Wu, C. Quartz Crystal Microbalance Studies on Conformational Change of Polymer Chains at Interface. *Macromol. Rapid Commun.* **2009**, *30*, 328–335.
- (5) Moya, S. E.; Brown, A. A.; Azzaroni, O.; Huck, W. T. S. Following Polymer Brush Growth Using the Quartz Crystal Microbalance Technique. *Macromol. Rapid Commun.* **2005**, *26*, 1117–1121.
- (6) Kanazawa, K.; Nam-Joon, C. Quartz Crystal Microbalance as a Sensor to Characterize Macromolecular Assembly Dynamics. *J. Sens.* **2009**, 1–17.
- (7) Marx, K. A. Quartz crystal microbalance: A Useful Tool For Studying Thin Polymer Films and Complex Biomolecular Systems at the Solution-Surface Interface. *Biomacromolecules* **2003**, *4*, 1099–1120.
- (8) Lubarsky, G. V.; Davidson, M. R.; Bradley, R. H. Hydration-Dehydration of Adsorbed Protein Films Studied by AFM and QCM-D. *Biosens. Bioelectron.* **2007**, *22*, 1275–1281.
- (9) Tlili, A.; Abdelghani, A.; Hleli, S.; Maaref, M. A. Electrical Characterization of a Thiol SAM on Gold as a First Step for the Fabrication of Immunosensors Based on a Quartz Crystal Microbalance. *Sensors* **2004**, *4*, 105–114.
- (10) Okajima, T.; Sakurai, H.; Oyama, N.; Tokuda, K.; Ohsaka, T. Electrical Equivalent-Circuit Parameters for Montmorillonite Clay

Film-Coated Quartz Crystal-Oscillators in Contact with Air, Moisture and Electrolyte-Solutions. *Electrochim. Acta* **1993**, *38*, 747–756.

(11) Muramatsu, H.; Tamiya, E.; Karube, I. Computation of Equivalent-Circuit Parameters of Quartz Crystals in Contact with Liquids and Study of Liquid Properties. *Anal. Chem.* **1988**, *60*, 2142–2146.

(12) Johannsmann, D. Viscoelastic Analysis of Organic Thin Films on Quartz Resonators. *Macromol. Chem. Phys.* **1999**, *200*, 501–516.

(13) Johannsmann, D. Viscoelastic, Mechanical and Dielectric Measurements on Complex Samples with the Quartz Crystal Microbalance. *Phys. Chem. Chem. Phys.* **2008**, *10*, 4516–4534.

(14) Ferry, J. D. *Viscoelastic Properties of Polymers*, 3rd ed.; Wiley: New York, 1980.

(15) Voinova, M. V.; Rodahl, M.; Jonson, M.; Kasemo, B. Viscoelastic Acoustic Response of Layered Polymer Films at Fluid-Solid Interfaces: Continuum Mechanics Approach. *Phys. Scr.* **1999**, *59*, 391–396.

(16) Degennes, P. G. Dynamics of Entangled Polymer-Solutions. 1. Rouse Model. *Macromolecules* **1976**, *9*, 587–593.

(17) Degennes, P. G. Dynamics of Entangled Polymer-Solutions. 2. Inclusion of Hydrodynamic Interactions. *Macromolecules* **1976**, *9*, 594–598.

(18) Harden, J. L.; Pleiner, H.; Pincus, P. A. A 2-Fluid Model for Surface-Modes on Concentrated Polymer-Solutions and Gels. *Langmuir* **1989**, *5*, 1436–1438.

(19) Milner, S. T. Dynamical Theory of Concentration Fluctuations in Polymer-Solutions under Shear. *Phys. Rev. E* **1993**, *48*, 3674–3691.

(20) Levine, A. J.; Lubensky, T. C. Response Function of a Sphere in a Viscoelastic Two-Fluid Medium. *Phys. Rev. E* **2001**, *63* (041510), 1–12.

(21) Johannsmann, D. *Piezoelectric Sensors*; Springer: Berlin, 2007; Vol. 5, p 49.

(22) Johannsmann, D.; Reviakine, I.; Richter, R. P. Dissipation in Films of Adsorbed Nanospheres Studied by Quartz Crystal Microbalance. *Anal. Chem.* **2009**, *81*, 8167–8176.

(23) Degennes, P. G. Conformations of Polymers Attached to an Interface. *Macromolecules* **1980**, *13*, 1069–1075.

(24) Antoniou, E.; Alexandridis, P. Polymer Conformation in Mixed Aqueous-Polar Organic Solvents. *Eur. Polym. J.* **2010**, *46*, 324–335.

(25) Auroy, P.; Auvray, L. Collapse-Stretching Transition for Polymer Brushes - Preferential Solvation. *Macromolecules* **1992**, *25*, 4134–4141.

(26) Fredrickson, G. H.; Pincus, P. Drainage of Compressed Polymer Layers - Dynamics of a Squeezed Sponge. *Langmuir* **1991**, *7*, 786–795.

(27) Daikhin, L.; Urbakh, M. Effect of Surface Film Structure on the Quartz Crystal Microbalance Response in Liquids. *Langmuir* **1996**, *12*, 6354–6360.

(28) Heuberger, M.; Balmer, T. E. The Transmission Interferometric Adsorption Sensor. *J. Phys. D: Appl. Phys.* **2007**, *40*, 7245–7254.

(29) Heuberger, M. The Extended Surface Forces Apparatus. Part I: Fast Spectral Correlation Interferometry. *Rev. Sci. Instrum.* **2001**, *72*, 1700–1707.

(30) Sannomiya, T.; Balmer, T. E.; Heuberger, M.; Voros, J. Simultaneous Refractive Index and Thickness Measurement with the Transmission Interferometric Adsorption Sensor. *J. Phys. D: Appl. Phys.* **2010**, *43* (405302), 1–9.

(31) Pasche, S.; De Paul, S. M.; Voros, J.; Spencer, N. D.; Textor, M. Poly(L-lysine)-graft-poly(ethylene glycol) Assembled Monolayers on Niobium Oxide Surfaces: A Quantitative Study of the Influence of Polymer Interfacial Architecture on Resistance to Protein Adsorption by ToF-SIMS and in Situ OWLS. *Langmuir* **2003**, *19*, 9216–9225.

(32) Urbakh, M.; Daikhin, L. Roughness Effect on the Frequency of a Quartz-Crystal Resonator in Contact with a Liquid. *Phys. Rev. B* **1994**, *49*, 4866–4870.

(33) Daikhin, L.; Gileadi, E.; Katz, G.; Tsionsky, V.; Urbakh, M.; Zagidulin, D. Influence of Roughness on the Admittance of the Quartz Crystal Microbalance Immersed in Liquids. *Anal. Chem.* **2002**, *74*, 554–561.

(34) McHale, G.; Newton, M. I. Surface Roughness and Interfacial Slip Boundary Condition for Quartz Crystal Microbalances. *J. Appl. Phys.* **2004**, *95*, 373–380.

(35) McHale, G. R. P.; Evans, C. R.; Shirtcliffe, N. J.; Elliott, S. J.; Newton, M. I. Sensor Response of Super-hydrophobic Quartz Crystal Resonators. Frequency Control Symposium. *IEEE Int.* **2008**, 698–704.

(36) Muller, M. T.; Yan, X. P.; Lee, S. W.; Perry, S. S.; Spencer, N. D. Lubrication Properties of a Brush-like Copolymer as a Function of the Amount of Solvent Absorbed within the Brush. *Macromolecules* **2005**, *38*, 5706–5713.

(37) Rixman, M. A.; Dean, D.; Ortiz, C. Nano-scale Intermolecular Interactions Between Human Serum Albumin and Low Grafting Density Surfaces of Poly(ethylene oxide). *Langmuir* **2003**, *19*, 9357–9372.

(38) Kawaguchi, T.; Hasegawa, M. Structure of Dextran-Magnetite Complex: Relation Between Conformation of Dextran Chains Covering Core and Its Molecular Weight. *J. Mater. Sci.: Mater. Med.* **2000**, *11*, 31–35.

(39) Basedow, A. M.; Ebert, K. H.; Feigenbutz, W. Polymer-Solvent Interactions - Dextrans in Water and DMSO. *Makromol. Chem.* **1980**, *181*, 1071–1080.

(40) Vaisman, I. I.; Berkowitz, M. L. Local Structural Order and Molecular Associations in Water DMSO Mixtures - Molecular-Dynamics Study. *J. Am. Chem. Soc.* **1992**, *114*, 7889–7896.

(41) Espinosa-Marzal, R. M.; Nalam, P. C.; Bolisetty, S.; Spencer, N. D. Impact of Solvation on Equilibrium Conformation of Polymer Brushes in Solvent Mixtures. *Soft Matter* **2012**, DOI: 10.1039/C3SM27726G.

(42) Pasche, S.; Textor, M.; Meagher, L.; Spencer, N. D.; Griesser, H. J. Relationship Between Interfacial Forces Measured by Colloid-Probe Atomic Force Microscopy and Protein Resistance of Poly(Ethylene Glycol)-grafted Poly(L-Lysine) Adlayers on Niobia Surfaces. *Langmuir* **2005**, *21*, 6508–6520.

(43) Huang, P.; Dong, A.; Caughey, W. S. Effects of Dimethyl Sulfoxide, Glycerol, and Ethylene Glycol on Secondary Structures of Cytochrome C and Lysozyme as Observed by Infrared Spectroscopy. *J. Pharm. Sci.* **1995**, *84*, 387–392.

(44) Van Oss, C. J. *Interfacial Forces in Aqueous Media*; Dekker Inc.: New York, 1994.

(45) Van Oss, C. J.; Arnold, K.; Good, R. J.; Gawrisch, K.; Ohki, S. Interfacial-Tension and the Osmotic-Pressure of Solutions of Polar Polymers. *J. Macromol. Sci., Chem.* **1990**, *A27*, 563–580.

(46) Antoniou, E.; Buitrago, C. F.; Tsianou, M.; Alexandridis, P. Solvent Effects on Polysaccharide Conformation. *Carbohydr. Polym.* **2010**, *79*, 380–390.

(47) Dinc, C. O.; Kibarar, G.; Guner, A. Solubility Profiles of Poly(ethylene glycol)/Solvent Systems. II. Comparison of Thermodynamic Parameters from Viscosity Measurements. *J. Appl. Polym. Sci.* **2010**, *117*, 1100–1119.

(48) Laloyaux, X.; Mathy, B.; Nysten, B.; Jonas, A. M. Surface and Bulk Collapse Transitions of Thermo responsive Polymer Brushes. *Langmuir* **2010**, *26*, 838–847.

(49) Muller, M. T.; Yan, X. P.; Lee, S. W.; Perry, S. S.; Spencer, N. D. Lubrication Properties of a Brush-like Copolymer as a Function of the Amount of Solvent Absorbed Within the Brush. *Macromolecules* **2005**, *38*, 5706–5713.

(50) Lai, P. Y.; Halperin, A. Polymer Brushes in Mixed-Solvents - Chromatography and Collapse. *Macromolecules* **1992**, *25*, 6693–6695.

(51) Please note that the initial frequency shifts and the areal solvation for PLL-g-PEG in HEPES solution in ref 49 and in our current paper do not match, in spite of the similar copolymer architecture. After consulting with the coauthors of ref 49, we found that they used the third overtone ($n = 3$) to estimate the frequency shifts and the net mass of the polymer film and thus these values are different from those we obtain (at $n = 9$). If similar overtones were used, the results from both the papers would show similar film thickness values for PEG brushes in HEPES solutions."

(52) Ben-Naim, A. Preferential Solvation in Two- and in Three-Component Systems. *Pure Appl. Chem.* **1990**, *62*, 25–34.

(53) Marcus, Y. Preferential Solvation in Mixed-Solvents. 5: Binary-Mixtures of Water and Organic-Solvents. *J. Chem. Soc., Faraday Trans.* **1990**, 86, 2215–2224.

(54) Marcus, Y. Some Thermodynamic and Structural Aspects of Mixtures of Glycerol with Water. *Phys. Chem. Chem. Phys.* **2000**, 2, 4891–4896.

(55) Hao, J. K.; Cheng, H.; Butler, P.; Zhang, L.; Han, C. C. Origin of Co-nonsolvency Based on the Structure of Tetrahydrofuran-Water Mixture. *J. Chem. Phys.* **2010**, 132 (154902), 1–9.